Paper ID #36603

Development of a PIV system for a Junior Level Fluid Mechanics Lab

Dr. Chuck H. Margraves, University of Tennessee at Chattanooga
Prof. Kidambi Sreenivas, The University of Tennessee Chattanooga
Mr. Alec Blade

Development of a PIV system for a Junior Level Fluid Mechanics Lab

Alec Blade, Kidambi Sreenivas, and Chuck Margraves
The University of Tennessee Chattanooga

Abstract

The purpose of this project is to enhance students' understanding of fluid dynamics through both an analytical and experimental approach. To achieve this, a Particle Imaging Velocimetry lab (PIV) is being developed to teach a relatively common flow field measurement technique. Flow fields are being covered extensively in the lecture portion of the class. However, we believe implementing this technique in conjunction with the lecture will enhance our engineering students' understanding. The current design for incorporating PIV is a rotating system to simulate Taylor Couette flow. This includes a static inner cylinder and a rotating outer cylinder with water as the medium. A laser sheet is directed through the outer cylinder where the flow field can be measured on the cylinders' radial axes. During pre-lab, students will be introduced to the analytic solution, which they will then use to compare to experimental results. The analytic solution contains calculating Reynolds number, radius ratios, and azimuthal velocities. The current experimental results show less than a 10% difference for the majority of the Couette flow field. However, larger errors are occurring at the surfaces of each cylinder. This error is likely due to reflections at the surfaces of the cylinders and modifications to the current system are underway.

Keywords

Experiential Learning, Particle Image Velocimetry, Flow Visualization

Introduction

At the University of Tennessee Chattanooga, all mechanical, chemical, and civil, engineering students participate in a junior-level fluid mechanics lab as a corequisite to the Fluid Mechanics lecture. Over the years this lab has changed to better reflect what students are introduced to in the classroom, but one area that has been missing is the ability to evaluate the velocity field of a moving fluid experimentally through a visualization technique. During the lecture portion of the class, students are introduced to several velocity profiles (flow fields) for varying types of flows, ranging from the parabolic distribution for fully developed laminar flow in a round pipe, to the profile created by Couette flow, as introduced below. The purpose behind the work presented in this paper is to provide students with the opportunity to both analytically predict a velocity profile, and then experimentally confirm the accuracy of the expression, thus closing the gap between knowledge gained during the lecture and that observed in the lab.

Taylor-Couette Theory

Couette Flow occurs in viscous fluids located between two tangentially moving surfaces. It is named after Maurice Couette, who developed a concentric viscometer and presented evidence of different flow regimes during the circular flow within pipes. Geoffrey Taylor took this idea further by attempting to calculate the symmetrical disturbances in viscous fluids between opposite rotating cylinders. Ultimately his work served as critical proof for the accuracy of the Navier-Stokes equations and the no-slip boundary condition [1]. A typical way of analyzing Taylor-Couette flow is by calculating the azimuthal velocity. This can be quite difficult when the flow is turbulent, but the equations for steady flow are much simpler. The equations used to calculate the azimuthal velocity in steady Taylor-Couette flow are listed below as equations 1-3 [2].

$$v_\theta = Ar + \frac{B}{r} \tag{1}$$

$$A = \frac{\Omega_2 R_2^2 - \Omega_1 R_1^2}{R_2^2 - R_1^2} \tag{2}$$

$$B = \frac{(\Omega_1 - \Omega_2) R_1^2 R_2^2}{R_2^2 - r_1^2} \tag{3}$$

Azimuthal velocity is given by v_θ where A and B are governed by the radius and angular velocities of the cylinders, and r is the radius at which the azimuthal velocity is to be calculated. The inner cylinder radius is denoted by R_1 and its angular velocity is denoted by Ω_1. The outer cylinder radius is denoted by R_2 and its angular velocity is denoted by Ω_2.

It is important to note that Taylor-Couette flow has a wide range of flow regimes that depend on the Reynolds number and radius ratio of the cylinders. Once the flow develops vortices, the above equations can no longer be used. The work of Dong at Cambridge University shows that Taylor-Couette flow is laminar at a Reynolds number of 1000, but vortices begin to occur at a Reynolds number of 3000 [3; pg. 375 and 377]. The formulas used to calculate the Reynolds number and radius ratio, under the Taylor-Couette conditions, are supplied below as equations 4 and 5.

$$Re = \frac{R_1 \Omega (R_2 - R_1)}{\upsilon} \tag{4}$$

$$\eta = \frac{R_1}{R_2} \tag{5}$$

Reynolds number in Taylor-Couette flow is dependent on the inner and outer cylinder's radius, the outer cylinder's angular velocity, and the kinematic viscosity of the medium. The mentioned variables are denoted as R_1, R_2, Ω, and υ respectively.

Experimental Setup

PIV is an optical technique used primarily to capture instantaneous velocities of a flow field. This is done through the use of a fluid medium, seeding particles, a direct illumination source, and an image-capturing device. For this work the seeding particles are sized on the scale of micrometers and are neutrally buoyant, having similar densities to the fluid medium, in order to ensure that the particles remain suspended during visualization. Being neutrally buoyant also allows the particles to accurately mimic the behavior of the fluid medium's molecules thus providing an accurate representation of the flow field. The light source used in many PIV experiments is a laser sheet which is used to illuminate a specific area of the flow to be analyzed. Post-processing of the captured images involves an Eulerian approach where a concentration of particles is tracked from one frame to the next. The distance of particle movement across pixels is calibrated beforehand to the physical distance. The distance traveled between frames and the time between each frame allows for the direct calculation of velocity. It should be noted that for this project, only two-dimensional motion is captured, however stereographic PIV can extend this work into three dimensions by making use of a second camera.

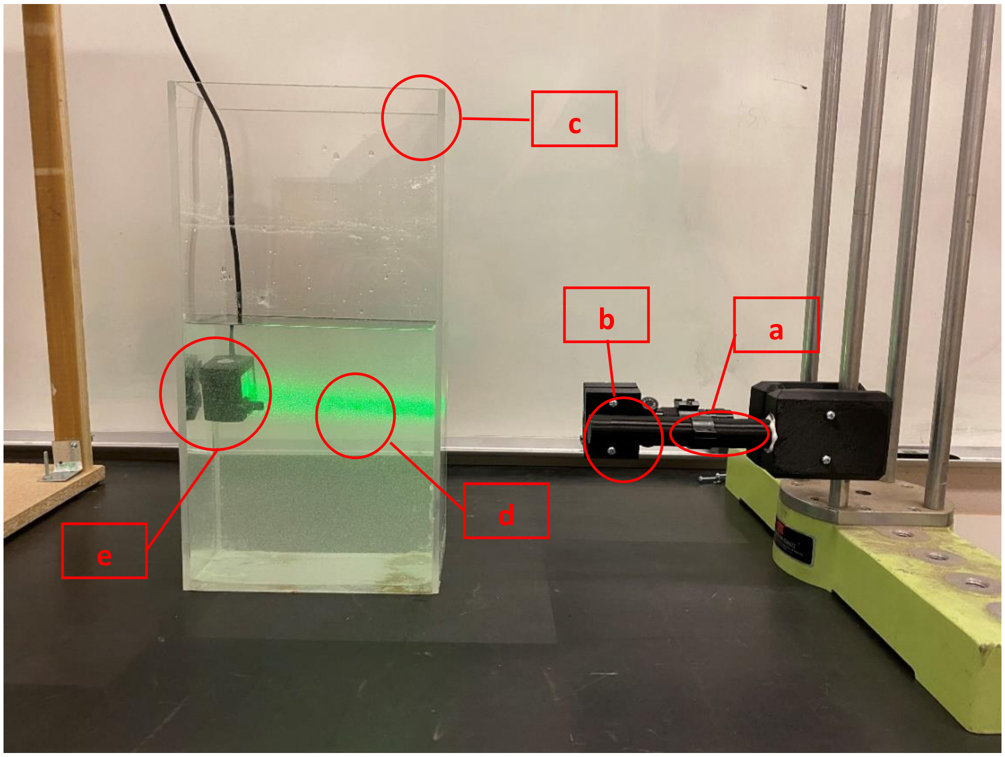

Fig. 1 Acrylic Tank Experimental Setup (a-laser, b-concaved lens housing, c-acrylic tank, d-laser sheet and seeding particles, e-submersible pump)

An initial experiment, shown in figure 1, was set up to verify the equipment selected was capable of illuminating a specific area and capturing the chosen particles. This work is similar to that completed by Professor Daniel Harris at Brown University. The experiment consisted of a rectangular acrylic tank, a submersible water pump, a water medium, polyamide particles, and a laser sheet. The acrylic tank had outer dimensions of $8\,in.(L) \times 4\,in.(W) \times 16\,in.(H)$ with a $^{1}/_{8}\ in.$ sheet thickness. The polyamide particles had a mean size of $55\ \mu m$ and a mean density of $1.2\ \frac{g}{cm^3}$. The density of the polyamide particles is $0.2\ \frac{g}{cm^3}$ greater than the density of water, however, this showed no significant effects on the results. The illumination source was a $532\ nm$ green laser that was dispersed into a laser sheet by a Plano-concaved cylinder lens with an effective focal length of $-12.50\ mm$. As mentioned above the laser sheet allowed for a two-dimensional flow field to be captured with a Panasonic Lumix GH5 Camera and $14 - 140mm$ lens. Figure 1 provides a visual representation of the described apparatus.

The first apparatus provided a means for testing our equipment. The laser sheet proved to be adequate at illuminating the polyamide particles. PIVlab [4], a software package within MATLAB, was also found to be an adequate tool for processing and analyzing the captured images. Slower moving particles were consistently tracked, but particles within the turbulent region were often lost. An analyzed frame of the first apparatus has been provided below in figure 2.

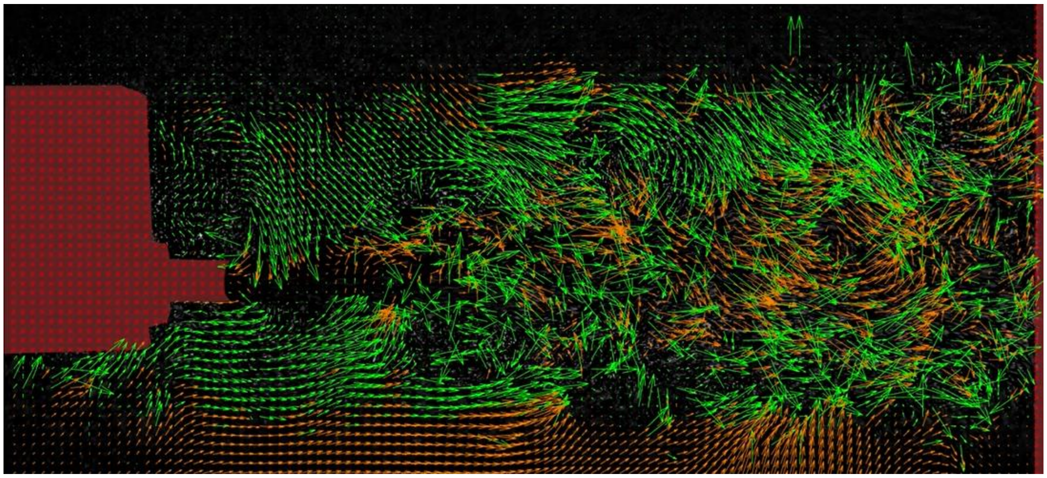

Fig. 2 First Apparatus Flow Field

The green vectors in figure 2 are the true calculated particle velocities while the orange vectors are interpolated values. This particular flow field did not have an exact solution to compare with. Thus, a second apparatus was determined to be constructed that would allow for non-turbulent flow and provide means of comparing analytical solutions to experimental results.

The second experimental setup was based on the theory of Taylor-Couette flow and included two concentric cylinders that were used with a medium of water between them. The inner cylinder was a PVC pipe with a radius of $0.024\,m$. The outer cylinder was an acrylic tank with a radius of $0.188\,m$. The inner cylinder was held static while the outer cylinder rotated with the use of a belt and a variable $12V$ DC electric motor. The same polyamide seeding particles used in the rectangular tank setup were used for particle tracking. Also, the same apparatus used to create the laser sheet in the rectangular tank setup was used for particle illumination. One improvement from our first experiment was the use of a Chronos 1.4 High Speed Camera with capabilities of $1{,}000\,fps$ and 1280×1024 image resolution. Figure 3, shown below, provides a visual representation of the described apparatus. The results from the setup are discussed in the results section.

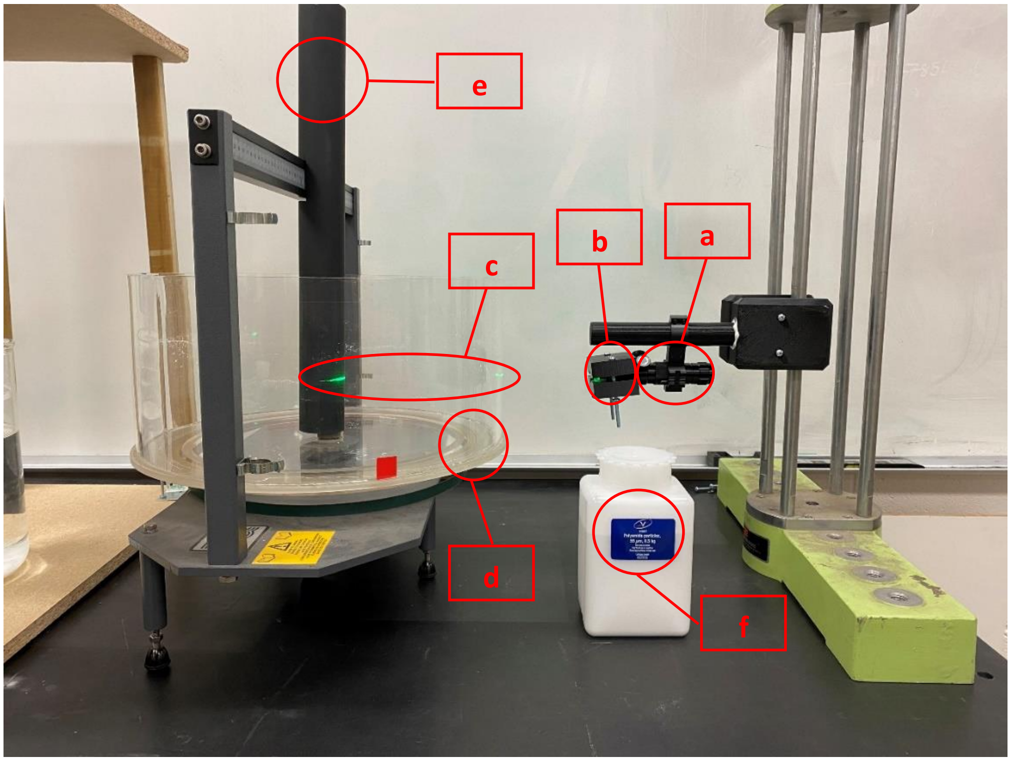

Fig. 3 First Taylor-Couette Experimental Setup (a-laser, b-concaved lens housing, c-laser sheet, d-outer cylinder, e-inner cylinder, f-seeding particles)

Experimental Results

The Taylor-Couette experiment allowed for the Reynolds number to be smaller than turbulent values [3]. The Reynolds number was found to be $Re = 2250$ and the radius ratio was $\eta = 0.127$. The calculations performed for the Reynolds number and radius ratio are shown below.

$$Re = \frac{(24\ mm)0.574\ \frac{rad}{s}(188 - 24\ mm)}{1.004\ \frac{mm^2}{s}} = 2250$$

$$\eta = \frac{24\ mm}{188\ mm} = 0.127$$

PIVlab was used to process 100 images captured at 120 fps. Each frame went through high-pass and contrast adaptive histogram equalization before submission of analysis to PIVlab. This allowed the algorithm to detect the seeding particles more effectively by adding contrast to the particles and reducing background noise. Figure 4 provides an example of a frame after processing.

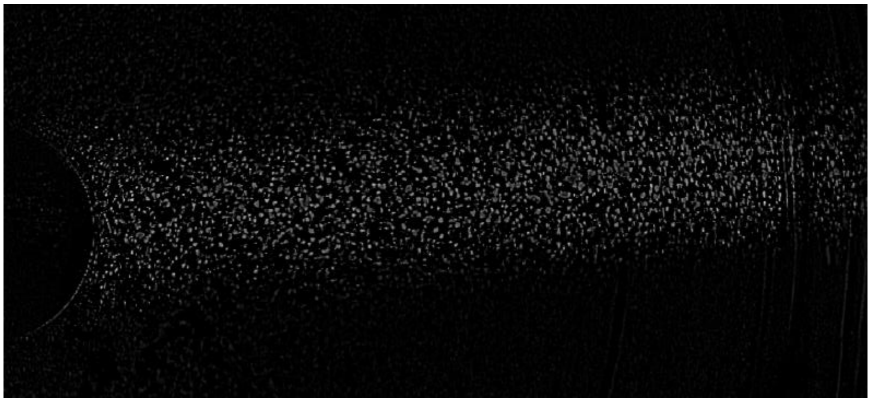

Figure 4 Post-Processing Frame Example

The PIV algorithm used for analyzing the processed images was the fast Fourier transform window deformation. The first-pass interrogation area was 120 pixels and was reduced by a factor of two for the second and third passes. Gauss 2x3-point fit was used for the sub-pixel estimator, and the correlation robustness was set to extreme. Ultimately, the results were averaged to produce the velocity flow field as shown below in figure 5. Velocity was taken along a polyline that was laid over the laser sheet placement.

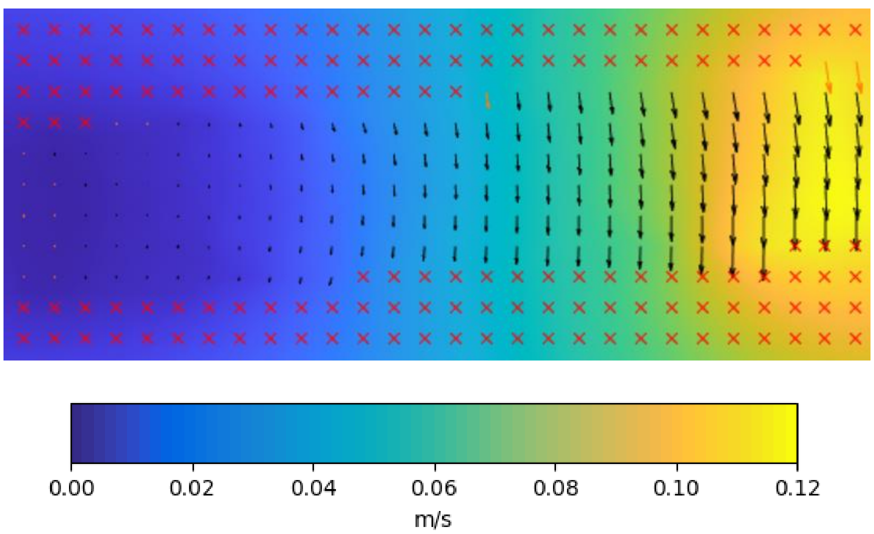

Fig 5 Averaged Velocity Flow Field

Analytical and Experimental Comparison

An analytical solution of the Taylor-Couette experiment was performed using equations 1-3. The radii of the cylinders were $R_1 = 0.024\ meters$ and $R_2 = 0.188\ meters$. The angular velocities of the cylinders were $\Omega_1 = 0.0$ and $\Omega_2 = 0.574\ \frac{rad}{s}$. This provided the following expression for analytically calculating the velocity field.

$$A = \frac{0.574\,\frac{rad}{s}\,(0.188\,m)^2 - 0.0\,\frac{rad}{s}\,(0.024\,m)^2}{(0.188\,m)^2 - (0.024\,m)^2} = 0.5835\,\frac{rad}{s}$$

$$A = \frac{\left(0.0 - 0.574\,\frac{rad}{s}\right)(0.024\,m)^2(0.188\,m)^2}{(0.188\,m)^2 - (0.024\,m)^2} = -0.003\,\frac{m^2}{s}$$

$$v_\theta = 0.5835\,\frac{rad}{s}\,(r) + \frac{-0.003\,\frac{m^2}{s}}{r}$$

The results of the experiment and analytical solution are plotted together in figure 6. 75% of the experimental results were below 10% difference when compared to the analytical solution. The 25% that were above 10% difference were either located at the inner cylinder surface or the outer cylinder surface. This is most likely due to the laser sheet reflecting off the cylinders' surfaces and disrupting the visualization of the seeding particles. The largest difference was at a radius of 0.024 resulting in a 74% variation. Overall, the inner 75% of the flow field held high agreement and followed the increasing velocity trend as set by the analytical solution.

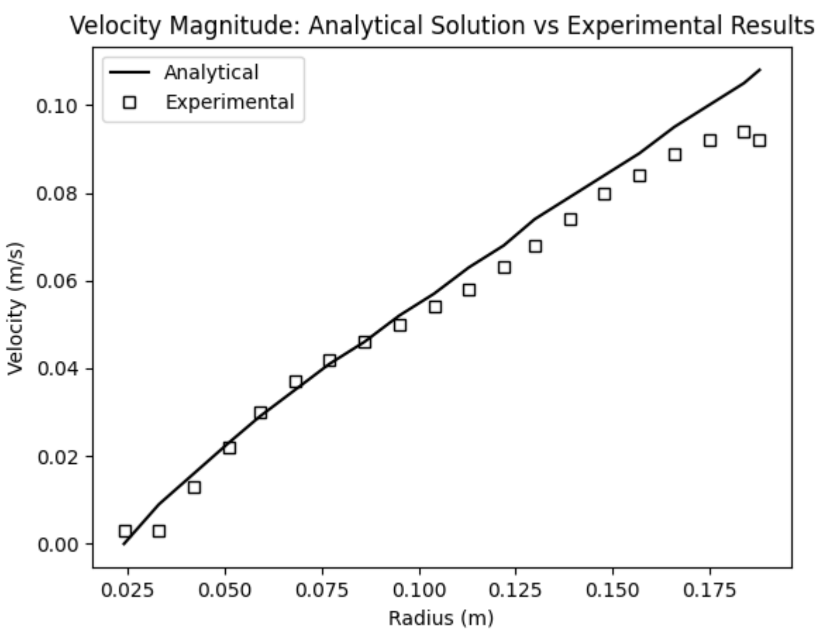

Radius	Solution (m/s)	Experiment (m/s)	Percent Error
0.024	0.002	0.003	74%
0.033	0.009	0.003	63%
0.042	0.016	0.013	22%
0.051	0.023	0.022	5%
0.059	0.029	0.030	3%
0.068	0.035	0.037	6%
0.077	0.041	0.042	3%
0.086	0.046	0.046	2%
0.095	0.052	0.050	4%
0.104	0.057	0.054	6%
0.113	0.063	0.058	8%
0.122	0.068	0.063	8%
0.130	0.074	0.068	7%
0.139	0.079	0.074	6%
0.148	0.084	0.080	6%
0.157	0.089	0.084	6%
0.166	0.095	0.089	6%
0.175	0.100	0.092	8%
0.184	0.105	0.094	11%
0.188	0.108	0.092	15%

Fig. 6 Analytical Solution vs Experimental Results

Conclusion and Recommendations

Despite some discrepancies at the edge of the experimental results, good agreement was found between the analytical and experimental findings. Within 75 % of the field, the average difference was less than 10%. We are currently working on improvements to the system in order to alleviate the error at the edges, including ways of reducing glare that may be affecting our results. In the future, we believe this apparatus will provide a significant improvement to our lab, as well as enhance students' understanding of flow fields in general. We are considering examining other flow fields such as the parabolic distribution for fully developed laminar flow in a round pipe, and possible flow over external surfaces in our water tunnel.

While we plan to only have one or two apparatus for the current setup, there should be considerable opportunity for all students to interact with the system, due to the short duration of the experiment. If we are successful in setting up differing experiments, with varying flow fields, we believe all students will be greatly impacted in their understanding of both this experimental technique, as well as the theoretical knowledge of this important aspect of fluid mechanics.

References

[1] Russell J. Donnelly. 1991. "Taylor-Couette Flow: The Early Days." *Physics Today 44: 32-39. https://doi.org/10.1063/1.881296.*

[2] Geoffrey I. Taylor. 1923. "VIII. Stability of a Viscous Liquid Contained Between Two Rotating Cylinders." *Philosophical Transactions of the Royal Society of London. Series A, Containing Papers of a Mathematical or Physical Character:* 289-343*. https://doi.org/10.1098/rsta.1923.0008.*

[3] S. Dong. 2007. "Direct Numerical Simulation of Turbulent Taylor-Couette Flow." Cambridge University Press. Volume 587: 373-393. https://doi.org/10.1017/S0022112007007367.

[4] PIVlab - Digital Particle Image Velocimetry Tool for MATLAB, https://pivlab.blogspot.com/; Accessed 01/13/2023.